PROCEEDINGS OF SPIE

SPIEDigitalLibrary.org/conference-proceedings-of-spie

Integrating image analysis with single cell RNA-seq data to study podocyte-specific changes in diabetic kidney disease

Darshana Govind, Saber Meamardoost, Rabi Yacoub, Rudiyanto Gunawan, John Tomaszewski, et al.

Darshana Govind, Saber Meamardoost, Rabi Yacoub, Rudiyanto Gunawan, John E. Tomaszewski, Pinaki Sarder, "Integrating image analysis with single cell RNA-seq data to study podocyte-specific changes in diabetic kidney disease," Proc. SPIE 12039, Medical Imaging 2022: Digital and Computational Pathology, 120390Q (4 April 2022); doi: 10.1117/12.2614495

SPIE.

Event: SPIE Medical Imaging, 2022, San Diego, California, United States

Integrating image analysis with single cell RNA-seq data to study podocyte-specific changes in diabetic kidney disease

Darshana Govind[1], Saber Meamardoost[2], Rabi Yacoub[3], Rudiyanto Gunawan[2], John E. Tomaszewski[1], Pinaki Sarder[1,*]

[1]Department of Pathology and Anatomical Sciences,
[2]Department of Chemical and Biological Engineering,
[3]Department of Internal Medicine,
University at Buffalo, Buffalo, NY

*Address all correspondence to: Pinaki Sarder
Tel: 716-829-2265; E-mail: pinakisa@buffalo.edu

ABSTRACT

Podocyte injury plays a crucial role in the progression of diabetic kidney disease (DKD). Injured podocytes demonstrate variations in nuclear shape and chromatin distribution. These morphometric changes have not yet been quantified in podocytes. Furthermore, the molecular mechanisms underlying these variations are poorly understood. Recent advances in omics have shed new lights into the biological mechanisms behind podocyte injury. However, there currently exists no study analyzing the biological mechanisms underlying podocyte morphometric variations during DKD. First, to study the importance of nuclear morphometrics, we performed morphometric quantification of podocyte nuclei from whole slide images of renal tissue sections obtained from murine models of DKD. Our results indicated that podocyte nuclear textural features demonstrate statistically significant difference in diabetic podocytes when compared to control. Additionally, the morphometric features demonstrated the existence of multiple subpopulations of podocytes suggesting a potential cause for their varying response to injury. Second, to study the underlying pathophysiology, we employed single cell RNA sequencing data from the murine models. Our results again indicated five subpopulations of podocytes in control and diabetic mouse models, validating the morphometrics-based results. Additionally, gene set enrichment analysis revealed epithelial to mesenchymal transition and apoptotic pathways in a subgroup of podocytes exclusive to diabetic mice, suggesting the molecular mechanism behind injury. Lastly, our results highlighted two distinct lineages of podocytes in control and diabetic cases suggesting a phenotypical change in podocytes during DKD. These results suggest that textural variations in podocyte nuclei may be key to understanding the pathophysiology behind podocyte injury.

I. INTRODUCTION

Diabetic kidney disease (DKD) is the most common cause of kidney failure in the United States[1]. Podocyte injury and subsequent loss are hallmark phenomenon associated with DKD[2]. Following injury, podocytes demonstrate variations in nuclear shape and chromatin distribution[3]. Although such textural variations in cancerous cells[4] are often quantified in digital pathology via nuclear

Medical Imaging 2022: Digital and Computational Pathology, edited by John E. Tomaszewski, Aaron D. Ward, Proc. of SPIE Vol. 12039, 120390Q · © 2022 SPIE
1605-7422 · doi: 10.1117/12.2614495

texture analysis, these changes have not yet been quantified in podocytes. Furthermore, the molecular mechanisms underlying these variations in podocytes are poorly understood.

Recent advances in omics have enabled the screening of a vast array of genes and proteins, which has shed new lights into understanding the biological mechanisms behind cell injury[5,6]. However, there currently exists no study analyzing the biological mechanisms underlying podocyte morphometric variations during DKD. Thus, the aim of this study was to evaluate the diagnostic value of podocyte nuclear morphometrics and textural features during DKD and to simultaneously study the underlying pathophysiology behind these variations.

II. RESULTS

To analyze podocyte morphometrics and texture, first, we performed nuclear texture analysis of podocytes from whole slide images (WSIs) of renal tissue sections obtained from control and murine models of DKD. Second, to study the molecular level changes in podocytes during DKD, we extracted single cell RNA sequencing (scRNA-seq) data from these murine models. Finally, to track potential shifts in podocyte phenotype during DKD, we performed a dynamic analysis of the scRNA-seq data using Clustering and Lineage Inference in Single-Cell Transcriptional Analysis (CALISTA)[7], a tool developed to track dynamic changes between distinct subgroups of cells based on their gene expression levels.

Image-based results:

Quantitative analysis confirmed histological changes in diabetic mice: Quantitative analysis indicated that the diabetic glomeruli hypertrophied ($p < 0.0001$) up to 1.25-fold the size observed in control mice (Fig. 1). Additionally, a significant depletion in both absolute and relative count of podocytes were observed ($p < 0.0001$) in diabetic mice (Fig. 1).

Subpopulations were identified based on podocyte nuclear texture and morphometrics: The podocyte nuclear morphometrics and textural features demonstrated the presence of five subclusters of podocytes. These results suggested the heterogenous nature of podocytes which may potentially explain their varying response to injury.

Nuclear texture demonstrated a statistically significant difference in diabetic podocytes compared to control: The nuclear texture, quantified using the histogram of gradients (HoG) feature descriptor, a feature vector commonly used in computer vision to track localized textural variations, demonstrated a statistically significant ($p < 0.05$) difference in diabetic podocyte nuclei compared to control, suggesting that podocyte nuclear texture may be key to understanding the pathophysiology behind podocyte injury during DKD.

ScRNA-seq-based results:

Podocytes were identified based on cell-specific markers: ScRNA-seq data analysis revealed nineteen different cell types in the mouse kidney, from which podocytes were identified using cell-specific markers (*Nphs1, Nphs2,* and *Tcf21*).

Gene expressions also revealed five subpopulations of podocytes: The unsupervised clustering of the detected podocytes from both control and diseased cases indicated the presence of five subclusters of podocytes. Among the five detected clusters, two clusters demonstrated a clear

separation (cluster 0 vs cluster 2 in Fig. 2A) between control and disease cases. The differentially expressed genes between subcluster 0 and 2 indicated that the latter demonstrated elevated levels of *Rasl11a* (a small GTPase protein with a high similarity to Ras), suggesting the involvement of Ras pathway effectors, and *Tspan2* (a tetraspanin protein), which is associated with glucotoxicity and apoptosis in pancreatic beta cells in type 2 diabetes.

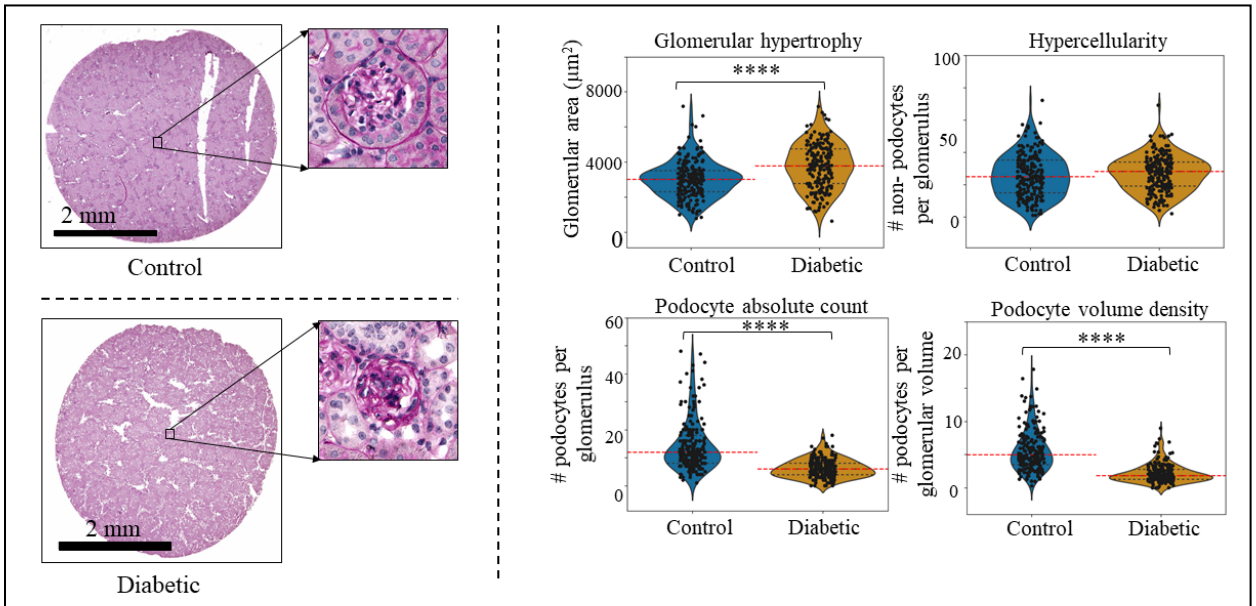

Fig. 1. Histological changes in diabetic mice. Quantitative analysis of renal tissue sections revealed statistically significant glomerular hypertrophy ($p < 0.0001$) as well as relative ($p < 0.0001$) and absolute ($p < 0.0001$) depletion of podocytes in diabetic mice.

Gene set enrichment analysis (GSEA) showed enrichment of epithelial mesenchymal transition (EMT) and apoptosis related genes in diabetic podocytes: GSEA was used to evaluate the gene expression data in podocytes. The results revealed EMT ($p < 0.05$) and apoptotic ($p < 0.05$) pathways in diabetic podocytes. These results highlight the varying biological mechanisms underlying podocyte injury.

Inference based on podocyte-specific changes in image-domain and scRNA-seq domain:

Podocytes nuclear morphometrics and textural data may provide insights into activation of EMT and apoptotic pathways during podocyte injury: The aforementioned image-based morphometric analysis revealed that podocyte nuclear texture was a key feature distinguishing diabetic from control podocytes. In tandem, the scRNA-seq highlighted EMT pathway (which is accompanied by dynamic changes in DNA methylation) and apoptotic pathway (which is accompanied by DNA fragmentation). These results suggest that podocyte nuclear morphometrics and textural features extracted from the WSIs may potentially aid in the identification of EMT or apoptosis-activated podocytes reflective of podocyte injury during DKD.

Dynamic analysis of podocyte-specific variations:

CALISTA-based analysis of the scRNA-seq data revealed two independent lineages in control and diabetic podocytes: Among the distinct subpopulations of podocytes identified in control and diabetic cases, the adjacent clusters were processed by CALISTA for dynamic analysis. The results demonstrated a dynamically distinct change in gene expressions in different podocyte subclusters, in both control and diabetic cases, indicating a phenotypical change in podocytes during DKD. As our next step, we will perform a similar study in the image-domain to track the gradual change in podocyte morphometrics with respect to disease severity.

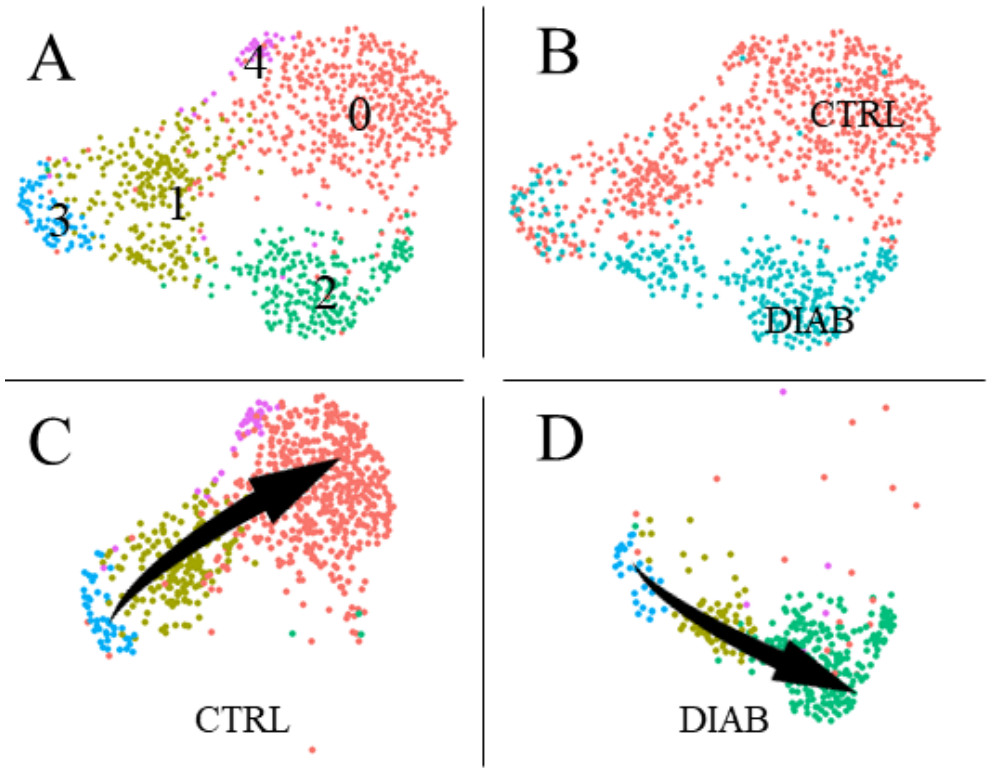

Fig. 2. Identified subclusters within podocytes and their dynamic analysis using CALISTA. (A) Re-clustering of previously identified podocyte subclusters, and **(B)** their respective disease status. The clusters separated by disease state (**(C)** control and **(D)** diabetic cases). The arrows indicate the direction of dynamic changes in individual subclusters, highlighting a phenotypical change in diabetic podocytes.

III. METHODS

From the mouse models, images of renal tissue sections were utilized to extract podocyte nuclear morphometrics. These sections were stained using periodic acid Schiff (PAS) counterstained with hematoxylin. To establish the ground truth for the hematoxylin-stained podocytes in the PAS WSIs, the same section was also stained using IHC markers labeling podocyte nuclei. To study the underlying pathophysiology, scRNA-seq data was extracted from the same mouse models.

Data acquisition:

Image data: Six formalin-fixed paraffin-embedded (FFPE) tissue sections of 2 µm thickness were obtained from wildtype control (n = 3) and db/db diabetic (n = 3) mouse kidneys and processed for staining. Each section was first stained using IHC markers labeling podocyte nuclei and imaged using Brightfield 40x oil on Leica Aperio VERSA 200 Whole Slide Scanner (Leica Biosystems Inc., Buffalo Grove, IL). Next, the IHC markers were bleached, and the sections were post-stained using PAS Stain Kit (ab150680, Abcam, Cambridge, UK) and counterstained with hematoxylin. The slides were then imaged using the same scanner. For labeling podocytes, p57 antibody was used as the primary and rabbit specific HRP/AEC chromogen (ab64260) (Abcam, Cambridge, UK) was used as the secondary antibody.

ScRNA-seq data: The 10x Genomics Chromium platform was used for extracting scRNA-seq data from the mouse kidneys. A total of 26,495 control cells (using aggregated cells from 3 mice) were sequenced to a depth of 15,218 reads per cell and 794 median genes per cell. A total of 63,209 diabetic mouse cells (using cells separately from 3 mice) were sequenced to a depth of 22,317 reads per cell and 512 median genes per cell. The output from 10X Genomics Cellranger version 3.0.1 pipeline was used as input into the R analysis package Seurat version 3.1.1. For quality control, the number of genes detected in a cell (between 200 and 5000) and their mitochondrial

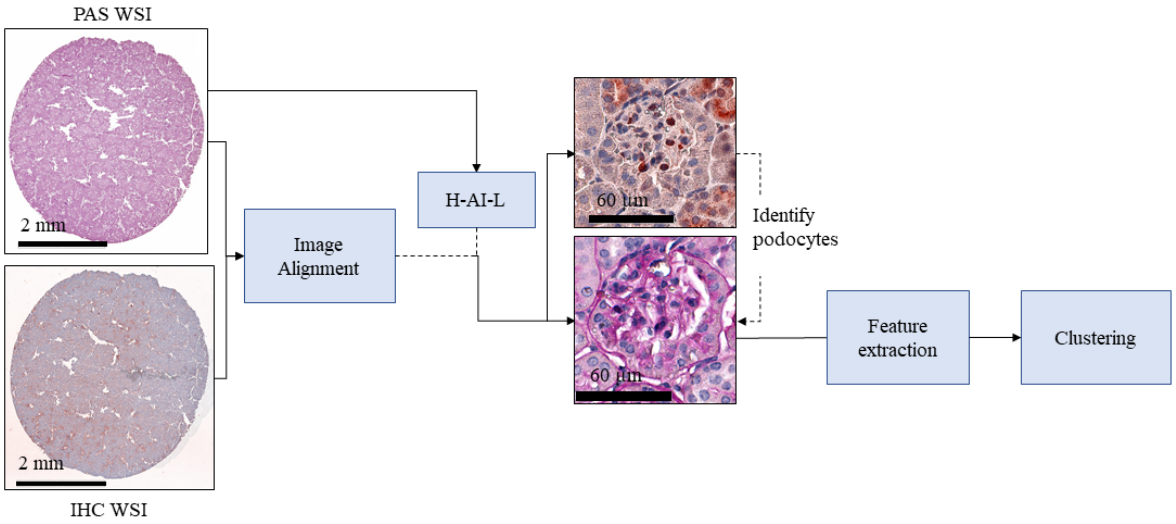

Fig. 3. Schematic pipeline for podocyte nuclei extraction in murine PAS-stained WSIs. The PAS and corresponding IHC-stained WSIs were first aligned using image registration. Next, the locations of glomeruli were identified using our H-AI-L pipeline. Once the glomeruli locations were identified, image patches containing glomeruli were extracted from the corresponding WSIs. Subsequently, the IHC-stained glomerular image patches were used as ground truth to identify and locate podocyte nuclei from the corresponding PAS images. Finally, the detected nuclei were extracted via morphological processing for subsequent morphometric quantification.

transcript load (>30%) were used to filter damaged or unwanted cells from analysis.

Image processing:

Podocyte nuclei detection and segmentation: To identify podocytes from the PAS WSIs, first, these WSIs were aligned with the corresponding IHC WSIs using a simple translation-based image registration. Next, prior to podocyte detection, we needed to identify glomerular locations within the WSIs. Thus, we utilized our previously published H-AI-L pipeline[8,9], a computational tool

designed to automatically detect glomeruli using a convolutional neural network (CNN). Once identified, image patches containing glomeruli were extracted from both WSIs. Subsequently, the p57-positive nuclei from the IHC glomerular image patches were used to identify podocyte nuclei in the PAS images, which were then extracted for morphometric quantification (Fig. 3).

Feature extraction: Several histological changes have been associated with DKD such as glomerular hypertrophy[10]. This increase in glomerular size leads to a relative depletion in podocyte densities, which progressively worsens with increasing disease severity[10]. Additionally, diseased glomeruli display mesangial expansion[11], a hallmark feature indicated by an increase in PAS-positive regions in the glomerulus. Apart from these glomerulus-level changes, individual podocytes undergo morphometric changes[12]. These changes are often accompanied by variations in chromatin distributions within the nuclei. To quantify these biological characteristics of podocyte nuclei along with the DKD-associated changes in the glomeruli, three distinct types of features were extracted from the detected podocyte nuclei: 1) standard morphological features of podocyte nuclei (to quantify their shape and size), 2) textural features of podocyte nuclei generated using histogram of gradients (HoG) feature descriptor (to quantify variations in chromatin distributions), and 3) local information of individual podocyte nuclei with respect to the glomerulus (i.e., proximity to the glomerular center). Furthermore, since the location of individual podocytes vary within the glomerulus, each of them may be subject to different levels of environmental stress leading to differences in morphological characteristics. Thus, to extract local information, the proximity of each podocyte nucleus to glomerular centroid and boundary was extracted. Additionally, the glomerular compartmentalization algorithm by Ginley *et al*. *JASN*, 2019[13] was used to segment the mesangial area within the glomeruli. Subsequently, the percentage of mesangial pixels surrounding each podocyte nucleus in a two-pixel radius was quantified. These local features may aid in the identification of potential subgroups of podocytes which are more prone to injury based on their locations within the glomerulus.

ScRNA-seq. data analysis: After quality control (as detailed previously), the scRNA-seq data was normalized using the SCT normalization[14] technique, followed by dimensionality reduction and visualization using Principal Component Analysis (PCA) and UMAP (Uniform Manifold Approximation and Projection). Finally, a SNN (Shared Nearest Neighbor) graph method was utilized for the unsupervised clustering of cells. For GSEA, the R package fgsea was used. The input genes were ranked by their log-fold changes from the differential expression analysis and the reference gene sets were collected from the Molecular Signatures Database (MSigDB).

IV. CONCLUSION AND FUTURE WORK

Our results highlight that podocyte nuclear morphometrics and texture may be key to understanding the pathophysiology behind podocyte injury. In the future we will employ CALISTA to study the dynamic changes in image-based podocyte morphometrics to study potential subclusters of podocytes and DKD-induced morphological changes in podocytes. This type of study may pave way into more complex studies into analyzing podocyte specific morphological changes and their underlying biological mechanisms.

ACKNOWLEDGEMENT

This project was supported by NIH-NIDDK grant R01 DK114485 (PS), NIH-OD grant R01 DK114485 03S1 (PS), a glue grant (PS) from the NIH-NIDDK Kidney Precision Medicine Project

grant U2C DK114886 (Contact: Dr. Jonathan Himmelfarb), a multi-disciplinary small team grant RSG201047.2 (PS) from the State University of New York, a pilot grant (PS) from the University of Buffalo's Clinical and Translational Science Institute (CTSI) grant 3UL1TR00141206 S1 (Contact: Dr. Timothy Murphy), a DiaComp Pilot & Feasibility Project 21AU4180 (PS) with support from NIDDK Diabetic Complications Consortium grants U24 DK076169 and U24 DK115255 (Contact: Dr. Richard A. McIndoe), NIH-OD grant U54 HL145608 (PS; Contact: Dr. Kun Zhang and Dr. Sanjay Jain), and NIDDK grant R01 DK131189 (PS; Contact: Dr. Farzad Fereidouni).

REFERENCES

1 Duru, O. K., Middleton, T., Tewari, M. K. & Norris, K. The landscape of diabetic kidney disease in the United States. *Current diabetes reports* **18**, 1-13 (2018).

2 Nagata, M. Podocyte injury and its consequences. *Kidney international* **89**, 1221-1230 (2016).

3 Hishikawa, A. *et al.* Decreased KAT5 expression impairs DNA repair and induces altered DNA methylation in kidney podocytes. *Cell reports* **26**, 1318-1332. e1314 (2019).

4 Domoguen, J. K. L., Suarez, J. J. P. & Naval, P. C. in *2019 3rd International Conference on Imaging, Signal Processing and Communication (ICISPC).* 155-159 (IEEE).

5 Chung, J.-J. *et al.* Single-cell transcriptome profiling of the kidney glomerulus identifies key cell types and reactions to injury. *Journal of the American Society of Nephrology* **31**, 2341-2354 (2020).

6 Karaiskos, N. *et al.* A Single-Cell Transcriptome Atlas of the Mouse Glomerulus. *J. Am. Soc. Nephrol.* **29**, 2060, doi:10.1681/ASN.2018030238 (2018).

7 Papili Gao, N., Hartmann, T., Fang, T. & Gunawan, R. CALISTA: Clustering And Lineage Inference in Single-Cell Transcriptional Analysis. *Frontiers in bioengineering and biotechnology* **8**, 18 (2020).

8 Lutnick, B. *et al.* An integrated iterative annotation technique for easing neural network training in medical image analysis. *Nature machine intelligence* **1**, 112-119 (2019).

9 Lutnick, B., Manthey, D. & Sarder, P. A tool for user friendly, cloud based, whole slide image segmentation. *arXiv preprint arXiv:2101.07222* (2021).

10 Li, J. *et al.* Podocyte biology in diabetic nephropathy. *Kidney International* **72**, S36-S42 (2007).

11 Steffes, M. W., Østerby, R., Chavers, B. & Mauer, S. M. Mesangial expansion as a central mechanism for loss of kidney function in diabetic patients. *Diabetes* **38**, 1077-1081 (1989).

12 Xu, J. *et al.* Diabetes induced changes in podocyte morphology and gene expression evaluated using GFP transgenic podocytes. *International journal of biological sciences* **12**, 210 (2016).

13 Ginley, B. *et al.* Computational Segmentation and Classification of Diabetic Glomerulosclerosis. *J. Am. Soc. Nephrol.*, ASN.2018121259, doi:10.1681/ASN.2018121259 (2019).

14 Hafemeister, C. & Satija, R. Normalization and variance stabilization of single-cell RNA-seq data using regularized negative binomial regression. *Genome biology* **20**, 1-15 (2019).